

Self-Assembly of Copper(II) Ion-Mediated Nanotube and Its Supramolecular Chiral Catalytic Behavior

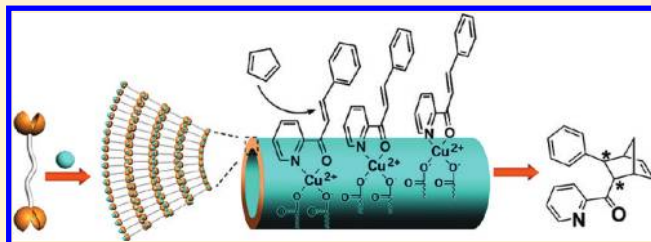
Qingxian Jin,[†] Li Zhang,[†] Hai Cao,[†] Tianyu Wang,[†] Xuefeng Zhu,[†] Jian Jiang,[‡] and Minghua Liu^{*,†}

[†]Beijing National Laboratory for Molecular Science, CAS Key Laboratory of Colloid, Interface and Chemical Thermodynamics, Institute of Chemistry, Chinese Academy of Sciences, Beijing, 100190, P. R. China

[‡]National Center for Nanoscience and Technology (NCNST), 100190 Beijing, P. R. China

 Supporting Information

ABSTRACT: Self-assembly of several low-molecular-weight L-glutamic acid-based gelators, which individually formed helical nanotube or nanofiber structures, was investigated in the presence of Cu^{2+} ion. It was found that, when Cu^{2+} was added into the system, the self-assembly manner changed significantly. Only in the case of bolaamphiphilic glutamic acid, *N,N'*-hexadecanedioyl-di-L-glutamic acid (L-HDGA), were the hydrogel formation as well as the nanotube structures maintained. The addition of Cu^{2+} ion caused a transition from monolayer nanotube of L-HDGA to a multilayer nanotube with the thickness of the tubular wall about 10 nm. For the other amphiphiles, the gel was destroyed and nanofiber structures were mainly formed. The formed Cu^{2+} -containing nanostructures can function as an asymmetric catalyst for Diels–Alder cycloaddition between cyclopentadiene and aza-chalcone. In comparison with the other Cu^{2+} -containing nanostructures, the Cu^{2+} -mediated nanotube structure showed not only accelerated reaction rate, but enhanced enantiomeric selectivity. It was suggested that, through the Cu^{2+} mediated nanotube formation, the substrate molecules could be anchored on the nanotube surfaces and produced a stereochemically favored alignment. When adducts reacted with the substrate, both the enantiomeric selectivity and the reaction rate were increased. Since the Cu^{2+} -mediated nanotube can be fabricated easily and in large amount, the work opened a new way to perform efficient chiral catalysis through the supramolecular gel.



INTRODUCTION

In recent years, the self-assembled organic nano- or micro-tubular structures have gained more and more interest¹ due to their attractiveness in the fields of nanofabrication,² guest encapsulation,³ drug delivery nanocarrier,⁴ and catalysis.⁵ Especially, nanotubular structures can provide a suitable and confined nanospace to increase efficiency or selectivity.⁶ In comparison with carbon nanotubes, the organic nanotubes have the advantages of being able to design and fabricate in a controlled manner and a large amount. In addition, tube formation is often related to chirality in many cases.⁷ Therefore, it is expected that the nanotube structures might be used as a scaffold to the chiral molecular recognition or even catalysis for the asymmetry reaction. Since lipid was found to form nanotubes in aqueous solution through self-assembly in the 1990s,⁸ many amphiphiles have been used for the fabrication of nano- or microtubular structures, including phospholipids,^{9,10} glycolipids,¹¹ and bolaamphiphiles.¹² Among them, bolaamphiphiles were widely studied, because one could control the nanotube dimensions including the inner and outer diameters, wall thickness, and inner and outer surface character,¹⁸ owing to its unique structure. Previously, we have investigated the self-assembly of a series of glutamic acid based lipids¹³ and successfully prepared helical nanotubes with monolayer thickness using bolaamphiphilic L-glutamic acid derivatives, *N,N'*-hexadecanedioyl-di-L-glutamic

acid (L-HDGA), and 1,4-dodecyloxy-bis(4-benzoyl-L-glutamic acid) (L-BECA)^{13b,c} as shown in Figure 1. In order to further functionalize these helical nanotubes, in this paper, we introduced Cu^{2+} ion into the system. For one reason, Cu^{2+} ion could help to stabilize the nanostructures. For the other, the Cu^{2+} could work as the center for some catalytic reactions. Interestingly, we have found that, with the introduction of the Cu^{2+} ion into those gels, L-HDGA still formed the nanotube structure, but the wall thickness was increased. However, BECA and hexadecanamide-glutamic acid (HGA) formed layered structures and nanofiber structures, respectively. More interestingly, the Cu^{2+} -mediated L-HDGA nanotube showed enhanced chiral catalytic behavior to the Diels–Alder cycloaddition between cyclopentadiene and aza-chalcone.^{14,15} Recently, due to rapid progress in knowledge of the self-assembly, many nanotube structures have been fabricated. In many cases, the nanotubes are chiral. However, there are scarcely any reports on chiral recognition and asymmetric catalytic activity for the lipid nanotubes. In this paper, we clearly demonstrated the possibility of Cu^{2+} -mediated chiral lipid nanotubes as a carrier for the asymmetric catalysis.

Received: August 9, 2011

Revised: September 30, 2011

Published: October 06, 2011

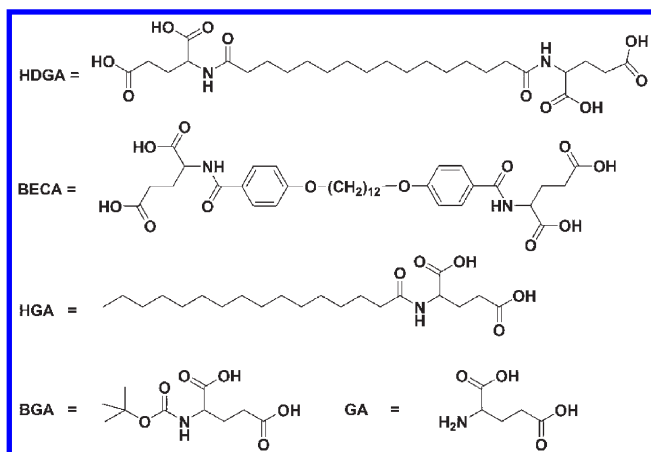


Figure 1. L-Glutamic acid-based derivatives used in this work. Among them, L-HDGA, L-HGA, and L-BECA can work as hydrogelator.

EXPERIMENTAL SECTION

Chemicals and Synthesis. Solid and liquid reagents were used as obtained from commercial suppliers without further purification; Milli-Q water (18.2 M Ω ·cm) was used in all cases. The glutamic acid derivatives: *N,N'*-hexadecanedioyl-di-L-glutamic acid (L-HDGA), *N,N'*-hexadecanedioyl-di-D-glutamic acid (D-HDGA), 1,4-dodecyloxy-bis-(4-benzoyl-L-glutamic acid) (L-BECA), and hexadecanamide-L-glutamic acid (L-HGA) were synthesized according to the previous report,¹³ and the structures were shown in Figure 1.

Cyclopentadiene was purchased from Aldrich. (*E*)-3-Phenyl-1-(pyridin-2-yl)prop-2-en-1-one (Aza-chalcones 2) was synthesized by an aldol condensation of benzaldehyde with 2-acetylpyridine, the same procedures reported by Engberts.¹⁴ ESI-MS: m/z calcd for [C₁₄H₁₁NO + H]⁺, 210; [C₁₄H₁₁NO + Na]⁺, 232. ¹H NMR (400 MHz, CDCl₃): δ 8.74–8.73 (d, 1H), 8.32–8.28 (d, J = 16 Hz, 1H), 8.19–8.17 (d, 1H), 7.95–7.91 (d, J = 16 Hz, 1H), 7.88–7.85 (t, 1H), 7.32–7.14 (d, 2H), 7.49–7.46 (t, 1H), 7.43–7.39 (m, 3H).

Self-Assembly Experiments and Diels–Alder Reactions. A mixture of glutamic derivations (0.01 mmol) and Cu(NO₃)₂·3H₂O (2.41 mg, 0.01 mmol) in H₂O (1 mL) was heated at 100 °C until the mixture was dissolved. Then, the resulting solution was cooled naturally and gelled or precipitated. Aza-chalcones 2 (20.9 mg, 0.1 mmol) was added to the solution or gels; after addition of freshly distilled cyclopentadiene, the reaction was stirred at room temperature, monitored by TLC (ethyl acetate/petroleum ether = 1:9). After the reaction finished, the mixture was purified by silica gel column chromatography (ethyl acetate/petroleum ether = 5:95) to give the Diels–Alder products 3 as yellow solid. ESI-MS: m/z calcd for [C₁₉H₁₇NO + H]⁺, 276; [C₁₉H₁₇NO + Na]⁺, 298. ¹H NMR (400 MHz, CDCl₃): δ 8.71–8.70 (d, 1H), 8.05–8.03 (d, 1H), 7.87–7.83 (t, 1H), 7.50–7.46 (t, 1H), 7.36–7.30 (m, 4H), 7.25–7.17 (m, 1H), 6.53–6.51 (t, 1H), 5.86–5.85 (d, 1H), 4.57–4.55 (t, 1H), 3.58 (s, 1H), 3.49–3.47 (d, 1H), 3.11 (s, 1H), 2.12–2.10 (d, 1H), 1.65–1.63 (d, 1H). The enantiomeric excess of the Diels–Alder products have been determined by HPLC analysis (Daicel Chiralcel-OD column, heptane/*i*-PrOH = 0.49:0.01, flow rate = 0.5 mL/min, λ = 254 nm): t_R = 12.616 min (exo major), t_R = 13.516 min (exo minor), t_R = 15.634 min (endo major), t_R = 18.316 min (endo minor).

Instruments and Methods. ¹H NMR spectra were recorded on a Bruker AV400 spectrometer. Electron spray ionization–mass spectrometry were recorded on Bruker APEXII instrument. Scanning electron microscopy (SEM) was performed on a Hitachi S-4800 FE-SEM microscope and transmission electron microscopy (TEM) images were

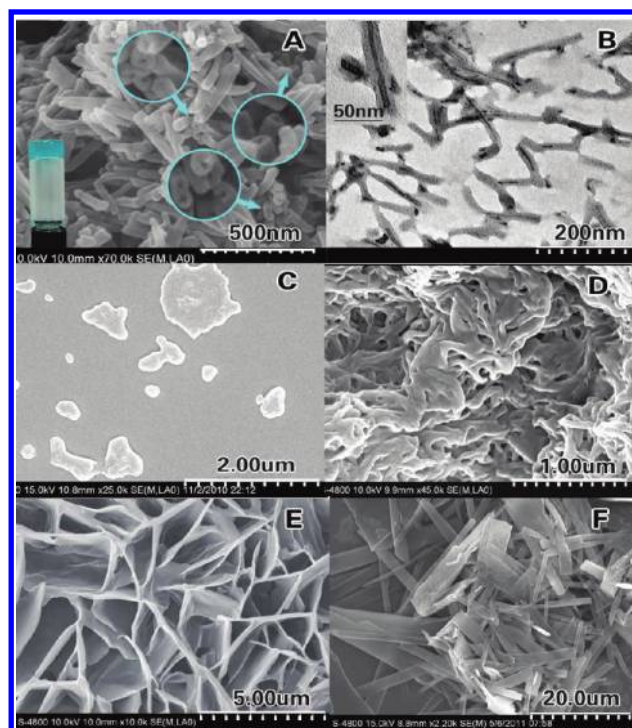


Figure 2. The morphology of Cu²⁺-L-HDGA xerogel: SEM image (A), TEM image (B); and the SEM image of Cu²⁺-L-HDGA hydrogel after addition of ethanol (C); morphology of the assembly of Cu²⁺-L-HGA (D), Cu²⁺-L-GA (E), and Cu²⁺-L-BECA (F).

obtained on a JEM 2100F operating at accelerating voltages of 15 and 200 kV, respectively. The fully aging gels or precipitates was cast onto single-crystal silica plates (Pt coated) and carbon-coated Cu grids (unstained), and the trapped solvent in gels or precipitates was evaporated at ambient conditions first, then vacuum-dried for 12 h for SEM and TEM measurements. Fourier transform infrared (FT-IR) spectra were recorded on a Bruker Tensor 27 FTIR spectrometer at room temperature. The KBr pellets made from the vacuum-dried xerogels were used for FT-IR spectra measurements. The quartz-plate-sustained xerogel films were used for X-ray diffraction (XRD) measurements, which was achieved on a Rigaku D/Max-2500 X-ray diffractometer (Japan) with Cu/K α radiation (λ = 1.5406 Å), which was operated at 45 kV, 100 mA. The enantiomeric excess was recorded on a Waters 1525 HPLC. The reaction kinetic measurements were performed on UV–vis spectroscopy (Jasco UV-550) monitoring the disappearance of the absorption of the Aza-chalcones at 25 \pm 0.1 °C. Typical concentrations were [Aza-chalcones] = 1 \times 10^{−2} M, [cyclopentadiene] = 5 \times 10^{−2} M, and [catalyst] = 1 \times 10^{−3} M.

RESULTS AND DISCUSSION

Copper(II)-Mediated Self-Assembly of the Bolaamphiphiles. Previously, we reported the self-assembly of L-HDGA and D-HDGA in aqueous solution, and helical nanotube structures were obtained through hydrogel formation.^{13a,c} In order to further functionalize the nanotube, we introduced Cu²⁺ into the nanotube because Cu(II) ion site has the catalytic behavior for certain reactions. Experimentally, Cu(NO₃)₂ and L-HDGA was dissolved in hot water and then cooled down to room temperature. The hydrogel containing Cu²⁺ ions was formed, with an obvious hyperchromatic effect, indicating the interaction of Cu²⁺ with L-HDGA.¹⁶ The xerogel of Cu²⁺-L-HDGA was subjected to

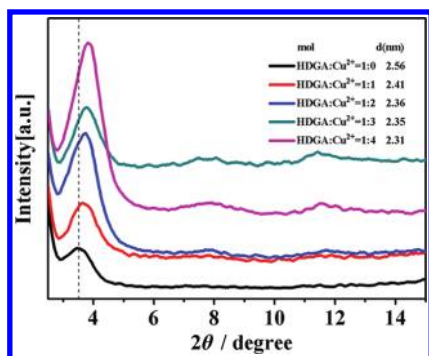


Figure 3. XRD pattern of xerogel of L-HDGA and Cu^{2+} /L-HDGA with the vary amount of Cu^{2+} .

scanning electron microscopy (SEM) and transmission electron microscopy (TEM) measurements. Figure 2A shows an SEM image of the xerogel of Cu^{2+} -L-HDGA. It has been found that, in the presence of Cu^{2+} , L-HDGA self-assembled into short nanostructures with polydispersity. The enlarged SEM image reveals that self-assembled nanostructures are hollow with width of 30–50 nm and length of 100–200 nm with open mouths (Figure 2A). TEM characterization taken from unstained xerogel further confirms that L-HDGA formed nanotube structures in the presence of Cu^{2+} , as shown in Figure 2B. TEM observation further reveals that the thickness of the tubular wall and diameter of the tube are about 10 and 10 nm, respectively. This thickness of the wall is much larger than the tubular wall of helical L-HDGA nanotube (ca. 3.0 nm), suggesting that the Cu^{2+} caused some changes during self-assembly. On the other hand, when Cu^{2+} ion was added into the other amphiphilic L-glutamic acid derivatives, no tubular structures were formed. As shown in Figure 2, the single head glutamic acid derivative L-HGA formed nanofibers, while the bolaamphiphile bearing hybrid spacers, which formed nanotubes in water,^{13d} formed large belts in the presence of Cu^{2+} . We speculated that such belts were made of the multilayer of L-BECA interacting with Cu^{2+} . However, the rigid aromatic rings close to the hydrophilic headgroups prohibited the layers from further rolling up into tubular structures. As a comparison for the following catalytic study, we also investigated the structures of the L-glutamic acid derivatives. These compounds formed no hydrogels with Cu^{2+} but formed precipitates. In the SEM observation, these precipitates showed nanostructures other than nanotubes.

As for L-HDGA, there are four carboxylic groups, which could possibly react with Cu^{2+} . In order to further characterize the nanotube structures and the effect of the amount of Cu^{2+} on the tubular structure, we have measured the XRD and FT-IR spectra for the Cu^{2+} mediated nanotubes.

Figure 3 shows the X-ray diffraction pattern of the xerogel from L-HDGA and Cu^{2+} /L-HDGA gels with various amount of Cu^{2+} . Well-defined patterns are observed for all these xerogels. For pure L-HDGA gels, only one diffraction peak is observed at 2θ values of 3.45, which corresponds to a layer distance of 2.56 nm. This value is slight smaller than that of the molecular length of L-HDGA (3.0 nm), indicating that L-HDGA formed a monolayer lipid membrane (MLM), with the alkyl chain tilted. When Cu^{2+} was introduced, the layer distances for the Cu^{2+} mediated nanotubes with different Cu^{2+} /L-HDGA ratios fell into 2.4–2.3 nm and decreased slightly with the increment of the ratio of Cu^{2+} /L-HDGA. This indicated that, upon reaction with

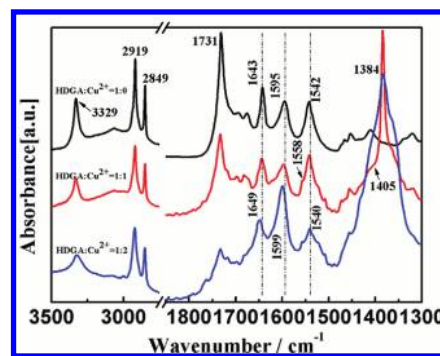


Figure 4. FT-IR spectra of xerogel of L-HDGA and Cu^{2+} -L-HDGA with different ratios.

Cu^{2+} , the alkyl chain in L-HDGA further inclined and all these nanotubes formed in a similar mechanism. Combined with the thickness of nanotube wall of 10 nm, estimated from TEM, we could suggest that four layers of L-HDGA together with the Cu^{2+} ions formed the wall of the nanotube. In addition, diffraction peaks become stronger with the increase of Cu^{2+} , especially for L-HDGA/ Cu^{2+} = 1:4, accompanied by the appearance of two new diffraction peaks (002 and 003). Nishimura et al. showed that the diffraction peak became weaker with increasing Cu^{2+} and eventually disappeared. They ascribed this to the transition from multi-bilayer tube to a single-bilayer tube.¹⁷ In the present case, it is just an opposite change from single layer nanotube to multi-layer nanotube. The change of the XRD patterns is in accordance with the literature and supported such changes.

Fourier transform infrared (FTIR) spectroscopy can provided more information on the binding, packing, and the interaction information between the L-HDGA and metal ions. Figure 4 showed the FT-IR spectra of the L-HDGA- Cu^{2+} gel. In L-HDGA gels, strong vibration bands are observed at 3329, 2919, 2849, 1731, 1643, 1595, and 1542 cm^{-1} . The band at 3329 cm^{-1} is ascribed to the N–H stretching with H-bonds, while the bands at 1643 and 1542 to the amide I and amide II, respectively. The bands at 1731, 1694, and 1675 can be assigned to the carbonyl stretching with the hydrogen bonds between carboxylic acid.^{13b} When Cu^{2+} was incorporated, the band at 1731 cm^{-1} significantly decreased and the band at 1595 cm^{-1} increased. The intensity of the bands at 3329 cm^{-1} decreased also. This was particularly obvious in the case of L-HDGA/ Cu^{2+} = 1:2 (The spectra for the L-HDGA/ Cu^{2+} = 1:3 and 1:4 are the same as the spectrum of 1:2, as shown in Supporting Information Figure S1), indicating that ionic interaction existed between copper ions and L-HDGA. In addition, a new shoulder band appeared at 1558 cm^{-1} , which could be assigned to the antisymmetric $V_{\text{as}}(\text{COO}^-)$.¹⁹ There is a strong band at 1384 cm^{-1} , which was due to the overlap of nitrate and $V_{\text{s}}(\text{COO}^-)$. These data indicated that Cu^{2+} could coordinate with the carboxylic acid.^{19,20} Thus, upon addition of the Cu^{2+} into the self-assembled system, both coordination and ionic interaction of the Cu^{2+} with bolaamphiphile changed the manner of assembly and multi-walled nanotubes were formed.

On the other hand, the L-HDGA gels showed the CH_2 asymmetric and symmetric vibration bands at 2919 and 2849 cm^{-1} , respectively, indicating all-trans configuration of the CH_2 group.²¹ When Cu^{2+} was incorporated, no shift of the CH_2 vibration bands was observed, showing that the stretch configuration of L-HDGA was essentially maintained.

Scheme 1. Illustration of the Assembly Mechanism of Cu^{2+} -L-HDGA Nanotubular Structure and Its Asymmetric Catalysis for Diels-Alder Reaction of Aza-Chalcone 2 with Cyclopentadiene 1

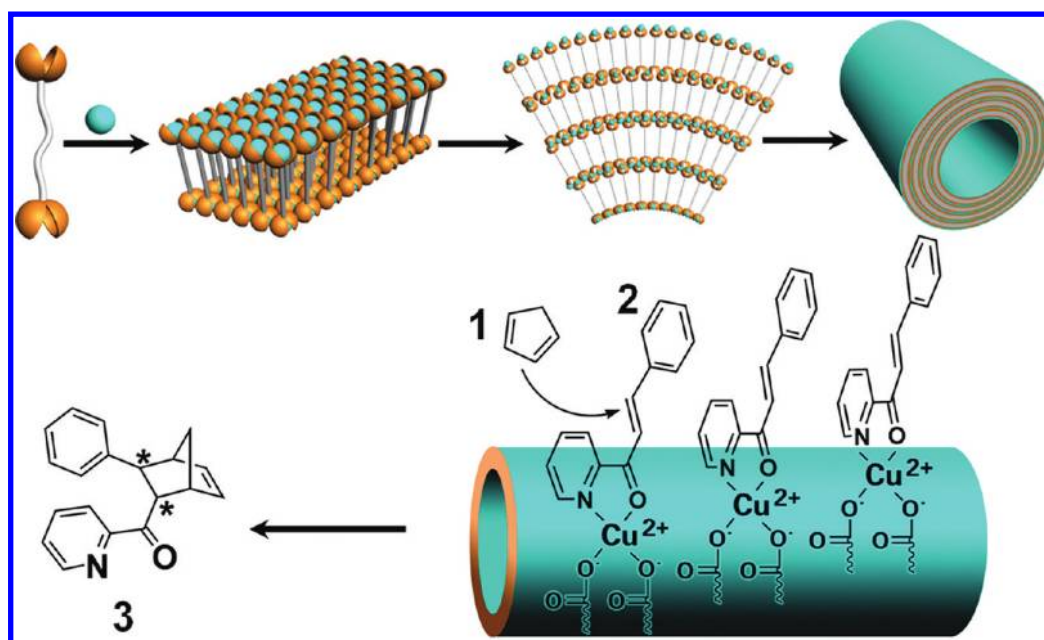


Table 1. Results of Diels–Alder reactions of 1 with 2 catalyzed by supramolecular catalysts

entry	ligand	yield ^a	dr ^b [endo/exo]	ee (%) ^b [endo]
1	L-HDGA	92%	95:5	47
2	L-HDGA	99%	93:7	1.2 ^c
3	L-HDGA	92%	93:7	2.2 ^d
4	L-HDGA	89%	97:3	51 ^e
5	D-HDGA	87%	96:4	−51
6	L-BECA	93%	95:5	7.3
7	L-HGA	92%	93:7	1.5
8	L-BGA	80%	92:8	4.5
9	L-GA	99%	95:5	5.3

^a Isolated yield. ^b By Chiral-HPLC. ^c Reaction was carried out in EtOH.

^d Reaction was added NaOH (4.0 equiv). ^e Reaction was carried out at 0 °C.

Chiral Catalytic Behavior. Asymmetry catalysis is one of the most important techniques in synthesizing chiral substances. While there is a large number of investigations into developing molecular catalyst for asymmetry reactions, the supramolecular catalyst has been attracting great interest recently.²² We have found that such Cu^{2+} -mediated nanotubes further showed asymmetric catalytic properties to the Diels–Alder reaction of aza-chalcone with cyclopentadiene, as shown in Scheme 1.

Experimentally, we dispersed the Cu^{2+} -L-HDGA nanotubes into the aqueous reaction system. After 24 h at room temperature, the reaction was completed. The product was isolated and enantiomeric excess of the products was determined by chiral-HPLC (Supporting Information Figures S2–3). The results are shown in Table 1. In order to compare the effect of the nanotube, we also investigated the catalytic behaviors of the other nanostructures formed by the L-glutamic acid derivatives shown in Figure 1 and Figure 2. The results indicated that the product is very dependent on the supramolecular structures of the catalyst.

Table 2. Results of Diels-Alder Reactions Catalyzed by Various Ratio L-HDGA- Cu^{2+}

Entry	Ratio [HDGA: Cu^{2+}]	Yield ^a	dr ^b [endo/exo]	ee (%) ^b [endo]
1	1:1	92%	95:5	47
2	1:2	95%	96:4	42
3	1:3	98%	96:4	41
4	1:4	99%	95:5	38
5	1:1 ^c	94%	95:5	55

^a Isolated yield. ^b By Chiral-HPLC. ^c CuCl_2 was used.

In the parallel experiments, the pristine amino acid was used to catalyze the D–A reaction as the chiral ligand of Cu^{2+} . Previous work has demonstrated that only aromatic amino acid, such as L-phenylalanine or L-tyrosine, can achieve about 30% ee value, while the aliphatic chain amino acids only showed very low enantioselectivity.¹⁴ We confirmed that the ee value of product was as low as 5% when we used L-glutamic acid as chiral ligand (Table 1 entry 9). Other derivatives including the Boc-L-glutamic acid (L-BGA) and the amphiphile with single head L-glutamic acid (Table 1 entries 7,8), and even the bolaamphiphile of BECA, which did not form nanotube structure with Cu^{2+} , showed enantioselectivity lower than 10% (Table 1 entries 6). However, when the reaction occurred in the presence of L-HDGA- Cu^{2+} nanotube, an impressive 47% ee (Table 1 entry 1) was obtained, which is considerably higher than the others. These results indicated that, although each L-glutamic acid based compound would not change its optical activity, only the nanotube formed with Cu^{2+} compound showed enhanced enantioselectivity for the catalytic D–A reaction. In addition, the product is related to the chirality of the nanotube. Previously, we reported that the bolaamphiphile from D-glutamic acid formed nanotubes with opposite handedness. When Cu^{2+} -mediated D-HDGA nanotube was used in the same manner, it resulted in product 3 with −51% ee.

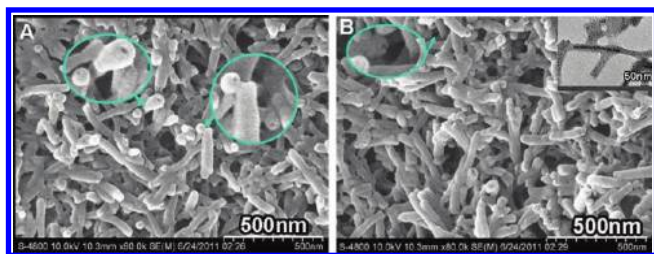


Figure 5. (A) SEM image of L-HDGA- $\text{Cu}(\text{NO}_3)_2$ xerogel at the ratio of 1:4; (B) SEM image of L-HDGA: CuCl_2 xerogel at the ratio of 1:1.

Effect of the Cu^{2+} Ions. Since the D–A reaction is related to the catalytic behavior of the Cu^{2+} , we have further investigated the effect of the amount of Cu^{2+} in the nanotube on the reaction. The result is listed in Table 2. With the increasing ratio of the Cu^{2+} in the nanotube, the yield was increased while the ee value showed a slight decrease. In addition, these ee values are much higher than those of the non-nanotube situation. The SEM observation revealed that the nanotubular structure of L-HDGA/ $\text{Cu}(\text{NO}_3)_2$ assemblies can be maintained even when the ratio of L-HDGA: $\text{Cu}(\text{NO}_3)_2$ was increased to 1:4, as shown in Figure 5. No matter whether the Cu^{2+} was less than or more than the number of the carboxylic acids, the catalytic reaction seemed to be not significantly affected. Besides, the assembly of CuCl_2 and L-HDGA also showed nanotubular structures (Figure 5B) and modest enantioselectivity (Table 2 entry 5). These results indicated that only those Cu^{2+} formed nanotube structures with L-HDGA would facilitate the enantioselective catalytic reaction.

The Cu^{2+} -L-HDGA nanotube not only enhanced the selectivity of D–A reaction, but also accelerated this reaction. The aza-chalcone exhibited a strong absorption peak at 325 nm in aqueous; upon the cycloaddition with cyclopentadiene, the adsorption band at 325 nm gradually decreased, while a new peak appeared at 280 nm, which was ascribed to product 3. Using this property, the reaction rate can be estimated. We plotted the decrease of absorption band at 325 nm as a function of reaction time in the presence of various Cu^{2+} -containing nanostructures, as seen in Figure 6B. It can be observed that, in comparison with the Cu^{2+} ions and other Cu^{2+} -mediated assemblies, the nanotube of L-HDGA- Cu^{2+} showed the fastest reaction rate.

From the results above, it is clearly seen that all the compounds containing the L-glutamic acid and Cu^{2+} showed different enantioselectivity and reactivity. Only the L-HDGA- Cu^{2+} assemblies with nanotubular structure showed enhanced enantioselectivity and accelerate the reaction.

The nanotube improved asymmetric catalysis and accelerated the D–A cycloaddition can be explained as Scheme 1. The interaction of Cu^{2+} and L-HDGA causes the formation of L-HDGA- Cu^{2+} nanotubes. In comparison with the L-HDGA alone, the addition of Cu^{2+} connected the neighboring L-HDGA molecules and formed a multilayer. Such layers rolled into the nanotube due to the chiral packing of the lamella structures. Upon nanotube formation, the chirality of the L-glutamic acid was transferred to the whole nanotube.^{13c} In this case, the Cu^{2+} ion was suggested to be aligned on the surface of the nanotube, which was subsequently worked as the catalytic sites, although it is difficult to observe such alignment directly even by TEM.²³ When aza-chalcone was mixed with the Cu^{2+} -incorporated nanotube, its carbonyl group and the pyridine nitrogen coordinated with the Cu^{2+} ion on the surface. Since the nanotube was chiral, it

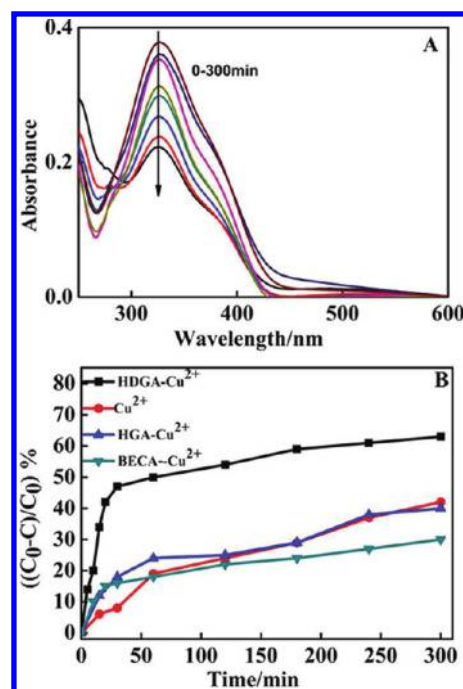


Figure 6. (A) UV–vis absorption spectra of D–A cycloaddition during the Cu^{2+} catalysis; (B) $((C_0 - C)/C_0)$ versus reaction time for the D–A cycloaddition over Cu^{2+} assemblies; C_0 and C are the absorption peaks at 325 nm initially and at time t .

will form a stereochemically favored environment for the next addition of cyclopentadiene. Due to a high density of catalytic sites²⁴ and chiral microenvironment to capture the substrate, the reaction proceeded with the enhanced enantioselectivity and accelerated reaction. The inner and outer surfaces of the nanotube might be similar in promoting the D–A reaction in the present case, since the nanotube is much larger in comparison with the molecules.

It should be further noted that the nanotubular structure is very important to enhance the enantioselectivity and the rate of the D–A reaction. In order to confirm this, NaOH was introduced into hydrogel, which had been used to increase the binding of chiral amino acid with Cu^{2+} .¹⁴ However, the introduction of NaOH into the system ruined the nanotube structure, and the enantioselectivity for the D–A reaction dropped significantly (Table 1 entry 3). Further, if we destroyed the nanotube structure by adding organic solvent such as ethanol (dissolving L-HDGA, Figure 2C) into the system, the enantioselectivity dropped significantly also (Table 1 entry 2). On the other hand, other nanostructures such as nanofiber and flakes have large surfaces, which can only show slight enantioselectivity since they could not form a stereochemically preferential microenvironment as the nanotube. It has been reported recently that the curvature can regulate some properties, such as ferroelectricity,^{25a} apparent $\text{p}K_a$,^{25b} and helical sense of peptide.^{25c} It seems that the curvature of the nanotube might be able to afford higher enantioselectivity of the nanotube than the other structures.

CONCLUSIONS

In conclusion, we have shown that the introduction of Cu^{2+} into a glutamic acid-based bolaamphiphilic lipid caused the formation of the nanotube with a multilayer wall. Such nanotubes showed enhanced-asymmetry catalytic behavior and accelerated

the asymmetric Diels–Alder cycloaddition between cyclopentadiene and aza-chalcone. The nanotubular structures, which provided a high density of catalytic sites and chiral microenvironment suitable for asymmetric reaction, benefit from the enantiomeric selectivity. Although a modest ee value was obtained, the enantiomeric selectivity of the product was still much higher than the control experiment without tubular structures in the identical condition. In addition, the Cu^{2+} -mediated nanotube structure showed a more predominant enantioselectivity than the other Cu^{2+} -mediated nanostructures such as nanofiber or flake. It is suggested that the alignment of the catalytic site on the surface of the nanotube and the stereochemical environment played an important role in producing such enantioselectivity. This result opened a new, efficient way for the supramolecular asymmetric catalysis. Further improvement on the ee value using the lipid nanotubes is underway.

■ ASSOCIATED CONTENT

S Supporting Information. Additional FT-IR spectra, HPLC separation chart for the enantiomers, and evaluation of the ee values. This material is available free of charge via the Internet at <http://pubs.acs.org>.

■ AUTHOR INFORMATION

Corresponding Author

*E-mail: liumh@iccas.ac.cn; Fax: 86-10-62569564; Tel: 86-10-82615803.

■ ACKNOWLEDGMENT

This work was supported by the Basic Research Development Program (2010CB833305), the National Natural Science Foundation of China (Nos. 20803084, 91027042), and the Fund of the Chinese Academy of Sciences. We also thank Prof. Yuantong Chen for providing the hexadecanedioic acid.

■ REFERENCES

- (a) Schnur, J. M. *Science* **1993**, 262, 1669. (b) Bong, D. T.; Clark, T. D.; Granja, J. R.; Ghadiri, M. R. *Angew. Chem., Int. Ed.* **2001**, 40, 988. (c) Jung, J. H.; Shinkai, S. *Top. Curr. Chem.* **2004**, 248, 223. (d) Shimizu, T.; Masuda, M.; Minamikawa, H. *Chem. Rev.* **2005**, 105, 1401. (e) Balbo Block, M. A.; Kaiser, C.; Khan, A.; Hecht, S. *Top. Curr. Chem.* **2005**, 245, 89. (f) Lee, H. Y.; Nam, S. R.; Hong, J. I. *Chem. Asian J.* **2009**, 4, 226. (g) Kameta, N.; Minamikawa, H.; Masuda, M. *Soft Matter* **2011**, 7, 4539.
- (a) Zhou, Y.; Shimizu, T. *Chem. Mater.* **2008**, 20, 625. (b) Llusar, M.; Sanchez, C. *Chem. Mater.* **2008**, 20, 782.
- (a) Shimizu, T. *J. Polym. Sci., Part A: Polym. Chem.* **2006**, 44, 5137. (b) Kameta, N.; Masuda, M.; Minamikawa, H.; Mishima, Y.; Yamashita, I.; Shimizu, T. *Chem. Mater.* **2007**, 19, 3553.
- (a) Meilander, N. J.; Yu, X. J.; Ziats, N. P.; Bellamkonda, R. V. *J. Controlled Release* **2001**, 71, 141. (b) Zarif, L. *J. Controlled Release* **2002**, 81, 7. (c) Frusawa, H.; Fukagawa, A.; Ikeda, Y.; Araki, J. A.; Ito, K.; John, G.; Shimizu, T. *Angew. Chem., Int. Ed.* **2003**, 42, 72.
- Martin, C. R.; Kohli, P. *Nat. Rev.* **2003**, 2, 37.
- Tang, Y.; Zhou, L.; Li, J.; Luo, Q.; Hung, X.; Wu, P.; Wang, Y.; Xu, J.; Shen, J.; Liu, J. *Angew. Chem., Int. Ed.* **2010**, 49, 3920.
- (a) Brizard, A.; Aimé, C.; Labrot, T.; Huc, I.; Berthier, D.; Artzner, F.; Desbat, B.; Oda, R. *J. Am. Chem. Soc.* **2002**, 129, 3754. (b) Hirst, A. R.; Smith, D. K.; Feiters, M. C.; Geurts, H. P. M. *Chem.—Eur. J.* **2004**, 10, 5901. (c) Hirst, A. R.; Smith, D. K.; Feiters, M. C.; Geurts, H. P. M. *Langmuir* **2004**, 20, 7070. (d) Ajayaghosh, A.; Praveen, V. K. *Acc. Chem. Res.* **2007**, 40, 644. (e) Pijper, D.; Feringa, B. L. *Soft Matter* **2008**, 4, 1349. (f) Lohr, A.; Würthner, F. *Chem. Commun.* **2008**, 2227. (g) Czajlik, A.; Beke, T.; Bottoni, A.; Perczelt, A. *J. Phys. Chem. B* **2008**, 112, 7956. (h) Ajayaghosh, A.; Praveen, V. K.; Vijayakumar, C. *Chem. Soc. Rev.* **2008**, 37, 109. (i) Kaiser, T. E.; Stepanenko, V.; Würthner, F. *J. Am. Chem. Soc.* **2009**, 131, 6719. (j) Yashima, E.; Maeda, K.; Iida, H.; Furusho, Y.; Nagai, K. *Chem. Rev.* **2009**, 109, 6102. (k) Isare, B.; Linares, M.; Zargarian, L.; Fermandjian, S.; Miura, M.; Motohashi, S.; Vanthuyne, N.; Lazzaroni, R.; Bouteiller, L. *Chem.—Eur. J.* **2010**, 16, 173. (l) Zhu, X. F.; Li, Y. G.; Duan, P. F.; Liu, M. H. *Chem.—Eur. J.* **2010**, 16, 8034.
- (a) Nakashima, N.; Asakuma, S.; Kim, J. M.; Kunitake, T. *Chem. Lett.* **1984**, 1709. (b) Schoen, Y. P. E. *Mol. Cryst. Liq. Cryst.* **1984**, 106, 371. (c) Yamada, K.; Ihara, H.; Ide, T.; Fukumoto, T.; Hirayama, C. *Chem. Lett.* **1984**, 1713.
- (a) Georger, J. H.; Singh, A.; Price, R. R.; Schnur, J. M.; Yager, P.; Schoen, P. E. *J. Am. Chem. Soc.* **1987**, 109, 6169. (b) Spector, M. S.; Selinger, J. V.; Singh, A.; Rodriguez, J. M.; Price, R. R.; Schnur, J. M. *Langmuir* **1998**, 14, 3493.
- (a) Thomas, B. N.; Corcoran, R. C.; Cotant, C. L.; Lindemann, C. M.; Kirsch, J. E.; Persichini, P. J. *J. Am. Chem. Soc.* **1998**, 120, 12178. (b) Thomas, B. N.; Cotant, C. L.; Lindemann, C. M.; Corcoran, R. C.; Cotant, C. L.; Kirsch, J. E.; Persichini, P. J. *J. Am. Chem. Soc.* **2002**, 124, 1227.
- (a) Frankel, D. A.; O'Brien, D. F. *J. Am. Chem. Soc.* **1991**, 113, 7436. (b) Frankel, D. A.; O'Brien, D. F. *J. Am. Chem. Soc.* **1994**, 116, 10057.
- (a) Fuhrhop, J. H.; Fritsch, D. *Acc. Chem. Res.* **1986**, 19, 130. (b) Fuhrhop, J. H.; Wang, T. *Chem. Rev.* **2004**, 104, 2901. (c) Meister, A.; Blume, A. *Curr. Opin. Colloid Interface Sci.* **2007**, 12, 138.
- (a) Zhan, C. L.; Gao, P.; Liu, M. H. *Chem. Commun.* **2005**, 462. (b) Gao, P.; Zhan, C. L.; Liu, M. H. *Langmuir* **2006**, 22, 775. (c) Jiang, J.; Wang, T. Y.; Liu, M. H. *Chem. Commun.* **2010**, 46, 7178. (d) Wang, T. Y.; Liu, M. H. *Langmuir* **2010**, 26, 18694. (e) Zhu, X. F.; Duan, P. F.; Zhang, L.; Liu, M. H. *Chem.—Eur. J.* **2011**, 17, 3429.
- (a) Otto, S.; Boccaletti, G.; Engberts, J. B. F. N. *J. Am. Chem. Soc.* **1998**, 120, 4238. (b) Otto, S.; Engberts, J. B. F. N. *J. Am. Chem. Soc.* **1999**, 121, 6798.
- (a) Roelfes, G.; Feringa, B. L. *Angew. Chem., Int. Ed.* **2005**, 44, 3230. (b) Roelfes, G.; Boersma, A. J.; Feringa, B. L. *Chem. Commun.* **2006**, 635. (c) Oltra, N. S.; Roelfes, G. *Chem. Commun.* **2008**, 6039. (d) Roe, S.; Ritson, D. J.; Garner, T.; Searle, M.; Moses, J. E. *Chem. Commun.* **2010**, 46, 4309.
- (a) Imaz, I.; Rubio-Martínez, M.; Saletta, W. J.; Amabilino, D. B.; MasPOCH, D. *J. Am. Chem. Soc.* **2009**, 131, 18222.
- Nishimura, T.; Matsuo, T.; Sakurai, K. *Phys. Chem. Chem. Phys.* **2011**, 13, 15899.
- (a) Kogiso, M.; Ohnishi, S.; Yase, K.; Masuda, M.; Shimizu, T. *Langmuir* **1998**, 14, 4978.
- Ohe, C.; Ando, H.; Sato, N.; Urai, Y.; Yamamoto, M.; Itoh, K. *J. Phys. Chem. B* **1999**, 103, 435.
- Huang, X.; Jiang, S. G.; Liu, M. H. *J. Phys. Chem. C* **2005**, 109, 114.
- (a) Umemura, J.; Cameron, D. G.; Mantsch, H. H. *Biochim. Biophys. Acta* **1980**, 602, 32. (b) Sapper, H.; Cameron, D. G.; Mantsch, H. H. *Can. J. Chem.* **1981**, 59, 2543.
- (a) Takacs, J. M.; Reddy, D. S.; Moteki, S. A.; Wu, D.; Palencia, H. *J. Am. Chem. Soc.* **2004**, 126, 4494. (b) Wang, X. S.; Wang, X. W.; Guo, H. C.; Wang, Z.; Ding, K. L. *Chem.—Eur. J.* **2005**, 11, 4078. (c) Breit, B. *Angew. Chem., Int. Ed.* **2005**, 44, 6816. (d) Reetz, M. T.; Jiao, N. *Angew. Chem., Int. Ed.* **2006**, 45, 2416. (e) Coquière, D.; Feringa, B. L.; Roelfes, G. *Angew. Chem., Int. Ed.* **2007**, 46, 9308. (f) Rodríguez-Llansola, F.; Miravet, J. F.; Escuder, B. *Chem. Commun.* **2009**, 7303. (g) Banerjee, S.; Das, R. K.; Maitra, U. *J. Mater. Chem.* **2009**, 19, 6649. (h) Escuder, B.; Rodríguez-Llansola, F.; Miravet, J. F. *New J. Chem.* **2010**, 34, 1044.
- (a) Nishida, N.; Yao, H.; Ueda, T.; Sasaki, A.; Kimura, K. *Chem. Mater.* **2007**, 19, 2831. (b) Zhou, Y. L.; Yang, M.; Sun, K.; Tang, Z. Y.; Kotov, N. A. *J. Am. Chem. Soc.* **2010**, 132, 6006.
- Guler, M. O.; Stupp, S. I. *J. Am. Chem. Soc.* **2007**, 129, 12082.

(25) (a) Nonnenmann, S. S.; Leaffer, O. D.; Gallo, E. M.; Coster, M. T.; Spanier, J. E. *Nano Lett.* **2010**, *10*, 542. (b) Wang, D. W.; Nap, R. J.; Lagzi, I.; Kowalczyk, B.; Han, S. B.; Grzybowski, B. A.; Szleifer, I. *J. Am. Chem. Soc.* **2011**, *133*, 2192. (c) Balamurugan, K.; Azhagiya Singam, E. R.; Subramanian, V. *J. Phys. Chem. C* **2011**, *115*, 8886.